Increasing Normal Modes Analysis Accuracy: The SPASIBA Spectroscopic Force Field Introduced into the CHARMM Program

P. Lagant,[†] D. Nolde,[‡] R. Stote,[§] G. Vergoten,[*,†] and M. Karplus[§,#]

UMR CNRS 8576 "Glycobiologie Structurale et Fonctionnelle", Université des Sciences et Technologies de Lille, 59655 Villeneuve d'Ascq, France, Shemyakin and Ovchinnikov Institute of Bioorganic Chemistry, Russian Academy of Sciences, Ul. Miklukho-Maklaya, 16/10 Moscow V-437,117871 GSP, Russia, Laboratoire de Chimie Biophysique, ISIS-UMR7006, Université Louis Pasteur, 67000 Strasbourg, France, and Department of Chemistry and Chemical Biology, Harvard University, Cambridge, Massachusetts 02138

Received: October 21, 2003

In the present work, the SPASIBA spectroscopic force field has been introduced into the CHARMM program. The SPASIBA force field combines the van der Waals and electrostatic interactions as originally found into CHARMM with Urey−Bradley−Shimanouchi terms for bond stretching, valence angle bending, torsional and improper torsional internal coordinates. SPASIBA has a vibrational spectroscopic origin, and it has largely proven its efficiency in reproducing experimental data such as vibrational wavenumbers, dipole moments, rotational barriers, conformational energy differences, and moments of inertia. The SPASIBA parameters have been included into CHARMM by way of a particular library which directly activates calculations of the specific energetic terms.

I. Introduction

The SPASIBA molecular mechanics force field is a spectroscopic molecular force field that treats bonds and bond angles by Urey−Bradley−Shimanouchi terms.[1,2] These terms have been previously combined with the torsional, van der Waals, and electrostatic terms of protein force fields, such as the AMBER[3] or the CHARMM force fields,[4] to provide a means to investigate the relationship between molecular spectra of proteins and their conformational properties. Previous studies have demonstrated that root-mean-square deviations between the observed and calculated vibrational frequencies for a large variety of chemical groups are in the 10−15 wavenumber range.[5−18] This level of agreement originates from the fact that the SPASIBA spectroscopic force field takes into account particular terms that have not been treated by other molecular mechanics force fields. These terms are directly related to the gem and/or tetrahedral redundancies. The SPASIBA force field includes geometric constraints that occur in bond angles and around tetrahedral atoms; this leads to the inclusion of several new terms, such as the F, F' and Kappa internal force constants, into the potential energy function. The addition of such terms to the potential energy function leads to a very good assignment for all the vibrational frequencies of methylene groups[6] and a correct determination of the gauche and trans conformations in alkanes and phospholipids.[15] In the current work, the SPASIBA force field was merged with the CHARMM potential energy function (SPASIBA/CHARMM); the internal energy terms are derived from the SPASIBA force field while the van der Waals and electrostatic terms are taken from the CHARMM force field.[4] The parametrization strategy was performed by iterative optimizations of the parameters leading to the best fit between the experimental and calculated vibrational wavenumbers using a SPASIBA-included version of the program AMBER[3]. The bonds, valence angles, dihedrals, and the particular parameters attached to the SPASIBA force field were directly transferred into the CHARMM program without any further refinement.

II. Methodology

II.a. Parametrization Methodology. For in-plane motions, the SPASIBA potential force field stands in three terms:

$$V_1 = \sum_{\text{bonds}} K(r_{ij} - r_{ij}^0)^2 + K'(r_{ij} - r_{ij}^0)$$

$$V_2 = \sum_{1-3} \frac{F}{2}(q_{ik} - q_{ik}^0)^2 + F'q_{ik}^0(q_{ik} - q_{ik}^0)$$

$$V_3 = \sum_{\text{angles}} Hr_{ij}^0\, r_{jk}^0(\theta_{ik} - \theta_{ik}^0)^2 + H'r_{ij}^0\, r_{jk}^0(\theta_{ik} - \theta_{ik}^0)$$

where r_{ij}^0, q_{ij}^0, and θ_{ik}^0 are related to the equilibrium values of the bonds, 1−3 nonbonded distances (gem), and valence angles respectively.[1−2] The q_{ik} values are themselves related to r_{ij}^0, r_{jk}^0, and θ_{ik}^0, and the linear terms K' and H' of this potential can be removed according to the linear relationships:

$$r_{ij}^0 K' + (r_{ij} - r_{ij}^0)F'_{ik} = 0$$

and

$$H'r_{ij}^0\ r_{jk}^0 + r_{ij}^0\ r_{jk}^0 \sin\theta_{ik}^0 F'_{ik} = 0$$

where $F' = -0.1F$, if the repulsion energy is of the r^{-9} type. This last term is very important in the estimation of the 1−3 repulsive interactions and is of the same order of magnitude as the repulsive force constants. The potential energy terms arising

* Corresponding author. E-mail: gerard.vergoten@univ-lille1.fr. Phone: 33320337150. Fax: 33320337279.
[†] Université des Sciences et Technologies de Lille.
[‡] Russian Academy of Sciences.
[§] Université Louis Pasteur.
[#] Harvard University.

10.1021/jp031178l CCC: $27.50
Published on Web 04/10/2004

from constraints around a central tetrahedral atom (Kappa) and angular (l), and trans−gauche (t−g) interactions have been also included in the new intramolecular potential energy term.

$$V_4 = V_l + V_{tg} + F_{red}{}^{*\text{Kappa}}$$

where

$$V_l = \sum_{i=1,2} l(\theta_{X_1CH_i} - \theta_0)(\theta_{X_2CH_i} - \theta_0) - \sum_{j=1,2} l(\theta_{X_jCH_1} - \theta_0)(\theta_{X_jCH_2} - \theta_0)$$

$$V_{tg} = f_{tg}(\theta_{ik} - \theta^0_{ik})(\theta_{jl} - \theta^0_{jl})$$

and

$$F_{red} = \sum_{i<j} a_{ij} d\theta_{ij} + \frac{1}{2}\sum_{i<1j} b_{ij} d\theta^2_{ij} + \frac{1}{2}\sum_{i,j<1k} c^k_{ij} d\theta_{ij} d\theta_{lk} + \frac{1}{2}\sum_{i\neq j\neq k\neq l} d^{kl}_{ij} d\theta_{ij} d\theta_{kl}$$

All coefficients and parameters given in these expressions have been discussed in detail in a former paper.[1]

The optimization of the specific force constants for several classes of compounds including *n*-alkanes, alkenes, alcohols, carboxylic acids, aldehydes, esters, ethers, aliphatic amino acid residues, phospholipids, and carbohydrates has been previously done[6−18] and led to a general root-mean-square deviation (rms) for vibrational wavenumbers that was on the order of 10−15 cm^{-1} presenting a significant improvement over other force fields currently used in molecular mechanics and molecular dynamics studies.

II.b. Torsional and Improper Potentials. The torsional potential energy function has the same analytical expression as the corresponding one used in the CHARMM program. For each class of chemical group examined under the SPASIBA force field, the torsional parameters have been carefully refined to obtain the correct potential energy barriers and differences between low-energy conformers.[1−2,6−18] The referring parameters have been included without modification into the SPASIBA/CHARMM library. In some series of chemical types of molecules, (alkanes, lipids, peptides, sugars), the dihedral potential energy function (PED) may be expressed according to single Fourier expansions depending on the order of the dihedrals. Additional SPASIBA "valence type" terms such as T−G (trans−gauche) have been shown to predict correctly the conformational behaviors and the relative energies between conformers.

Besides the energy differences between low-energy conformers, the dipole moments were considered as giving an approximate measure of the molecular geometries and, then, added in the description of the potential energy distributions.

The SPASIBA force field was primitively developed via its inclusion into the AMBER program[3] in which out-of-plane motions were treated along improper torsional energy functions. We kept this convenient form to treat out-of-plane deformations, as the transferability criterion to analogues of molecules containing such motions was found to be of good quality, especially in using isotopic substituents when reproducing the observed frequency shifts. Moreover, for the light hydrogen atoms a pure quadratic term would not be sufficient to take into account large out-of-plane motions for which anharmonic effects would be present.

The force field relative to the CHARMM program is principally devoted to the determination of the conformational and dynamical properties of proteins and organic molecules taken in bulk environments. The aim of SPASIBA was to introduce internal parameters for the molecule and to add adequate external perturbations (crystal, solvent interactions) according to the present environments. It can be seen below that the two methods are not mutually exclusive but, rather, that a good parametrization obtained from spectroscopic data brings a larger precision in the potential energy determination.

II.c. Merging the SPASIBA Force Field with the CHARMM Package. The SPASIBA force field has been merged with the CHARMM force field and incorporated into the CHARMM program. The specific parameters are read via a modified parameter file that includes the K, H and F (and F') terms and the specific Kappa, l_{CH2}, trans and gauche force constants that are calculated for every potential energy evaluation. The out-of-plane parameters deduced from the SPASIBA force field refinements were added in a similar way including the particular parameters referring to the improper dihedrals. The program was implemented in such a way that either the CHARMM parameters or the SPASIBA parameters could be used for the bond stretching, valence angle bending, torsional or improper torsional angles depending on the specific residue. When no corresponding SPASIBA parameters could be found, the corresponding CHARMM parameters are used by default. As introduced into the CHARMM program, the SPASIBA force field can be used to calculate bond stretching and in-plane bending contributions to the potential energy function as well as their first and second derivatives with respect to internal coordinates. The nonbonded and electrostatic parameters have not been modified in order to maintain this specific feature of the CHARMM program.

III. Results and Discussion

Potential energy minimization and the normal mode analyses have been performed for several small molecules that are characteristic of different chemical groups: peptides (NMA, *N*-acetyl-L-alanine), alkanes, ethers (methylethyl ether), thiols (ethanethiol), esters (methyl acetate), alkenes, alcohols (methanol and ethanol), and saccharides. As much as possible, direct comparison of the calculated wavenumbers and the potential energy distribution (PED) using the original CHARMM and SPASIBA/CHARMM force fields was performed.

III.a. *N*-Methylacetamide (NMA). NMA is one of the simplest models for a peptide as it contains a single peptide bond. This molecule adopts a trans conformation in the gas and liquid states.[19] The primitive values of the internal parameters given by Katz and Post for NMA in the crystal state[20] were corrected by Hamzaoui and Baert.[21] Theoretical values have been obtained from ab initio studies.[22] Table 1 gives the experimental, calculated wavenumbers and the potential energy distribution (PED) for NMA as calculated using both the SPASIBA and SPASIBA/CHARMM force fields.

For the SPASIBA calculations, the force constants were taken directly from the SPASIBA force field library as opposed to the force constants that were refined for the SPASIBA/CHARMM force field. Some differences between the current calculated values and those obtained in previous calculations[1] can be observed. These differences originate mainly from the fact that for the current calculations, nonbonded and electrostatic contributions were calculated using the CHARMM parameters (CHARMM22 in the c26a2 version). In general, a good

TABLE 1: NMA (*N*-Methylacetamide) Calculated and Experimental (exptl) Vibrational Wavenumbers (in cm^{-1}) and the Potential Energy Distribution[a]

exptl	SPASIBA		SPASIBA/CHARMM		CHARMM		ref 23
	71	τCT−C	90	τC−C + τN−C			
	96	τCT−N	107	τC−C + τN−C	100	δCN−CH$_3$	
	175	δCT−N−C	230	0.44δCNCT	151	τC−N	184
290$_L$	292	δCTNC + δ CTCN	298		290	δCN−CH$_3$ (N)	286
436$_L$	428	δC═O	428	δC═O	422	δC═O + νC−N	440
	570	γC═O			651	γC═O	587
628$_G$	620	δC═O	608	0.32δC═O + νCTC	531	0.44δC═O	591
	706	γNH	729	γN−H	775	0.75γN−H	696
	873	νC−N + νCT−C	868	νC−N + νCTC	749	0.31C−N + 0.1C−CH$_3$ (C)	801
973$_G$, 992$_L$	985	rCH$_3$	992	rCH$_3$ (C)	943	rCH$_3$ (N) + rCH$_3$ (C)	963
1043$_{G,L}$	1048	rCH$_3$	1040	rCH$_3$	1037	rCH$_3$ (N)	1037
	1096	νC−CT + rCH$_3$(N)	1076	rCH$_3$ (N)	1061	rCH$_3$ (N)	1075
	1096	νC−N + νCT−C	1089	νN−CH$_3$ + νCH$_3$−C + rCH$_3$			
1176$_L$, 1162$_L$	1160	νN−CH$_3$	1176	νN−CH$_3$	1186	0.36rCH$_3$ + 0.22δN−H + 0.16νC−N	1082
1263$_G$, 1299$_L$	1275	νC−N + νCT−C	1281	νC−N + νCT−C	1327	δCH3 (C) + 0.21δNH	1209
1374$_G$	1374	δsCH$_3$	1377	δsCH$_3$ (C)	1365	0.98δsCH$_3$ (C)	1395
1430$_G$	1438	δaCH$_3$	1420	δaCH$_3$ (N)	1386	δaCH$_3$ (N)	
	1443	δaCH$_3$	1437	δaCH$_3$ (C)	1365	δaCH$_3$ (C)	1402
1450$_L$	1446	δaCH$_3$	1449	δaCH$_3$ (C)	1396	δaCH$_3$ (C)	1407
1414$_L$	1500	δsN−CH$_3$	1452	δaCH$_3$ (N)	1421	δaCH$_3$ (N)	1428
1567$_L$	1563	δN−H + νC−N	1562	0.3νCN + 0.13νNC + 0.13δNH	1556	0.38δNH + 0.19νCN + 0.17νNCT	1614
1732$_G$, 1655$_L$	1665	νC═O	1665	0.75νC═O + 0.1νC−N	1666	0.69νC═O + 0.11νC−N	1693
	2912	νsCH$_3$	2910	νsCH$_3$(N)	2729	νsCH$_3$ (C)	2868
	2914	νsCH$_3$	2918	νsCH$_3$ (C)	2730	νaCH$_3$ (C)	2869
	2971	νaCH$_3$	2971	νaCH$_3$ (N)	2841	νaCH$_3$ (C)	2980
	2972	νaCH$_3$	2972	νaCH$_3$ (N)	2842	νsCH$_3$ (N)	2982
	2974	νaCH$_3$	2978	νaCH$_3$ (C)	2843	νaCH$_3$ (N)	2982
	2974	νaCH$_3$	2978	νaCH$_3$ (C)	2845	νaCH$_3$ (N)	2983
3300$_L$	3292	νN−H	3298	νN−H	3329	νN−H	3304
rms	10.6		17		38.2		42.6

[a] ν, stretching; δ, in-plane bending; τ, torsion; a and s, antisymmetric and symmetric coordinates; G, gas; L, liquid; rms in cm^{-1}.

agreement between the experimental and calculated vibrational frequencies was obtained with an rms of 17 cm^{-1} for the SPASIBA/CHARMM force field, while the SPASIBA force field gave an rms of 10 cm^{-1} and the CHARMM force field gave an rms of 38.2 cm^{-1}. For comparison, the experimental and calculated frequencies given by the Cornell et al. have also been included.[23]

The experimental enthalpy difference between the trans and cis conformers of NMA has been reported to be −2.3 kcal mol^{-1}.[24] Derreumaux and Vergoten found a value of −1.77 kcal mol^{-1} for the calculated enthalpy difference using a single 2-fold order for the amide torsion[1], and a similar value would be expected here.

III.b. *N*-Acetyl-L-alanine. The second model of a peptide is given by the alanyl dipeptide. NMR and electrical circular dichroism experiments have shown that, in water, this peptide preferentially adopts a hydrogen-bonded ring of the C7 equatorial type (C7$_{eq}$).[25] Monte Carlo and free-energy simulations have confirmed that the C7$_{eq}$ conformer is well stabilized in water as are several other conformers (C7$_{ax}$, C5, and helical conformations).[26] More recently, MacKerell et al.[4] calculated the relative energies of the C7$_{eq}$, C7$_{ax}$, and C5 conformers of this peptide using an empirical CHARMM force field and ab initio calculations at the HF/6-31G** level of theory. The introduction of the SPASIBA terms into the CHARMM program leads to a potential energy distribution among internal coordinates that is quite comparable to results given by Derreumaux and Vergoten (rms = 12.7 cm^{-1}).[1] In the present work, a somewhat larger rms (26 cm^{-1}) between the experimental and calculated vibrational frequencies was obtained in the gas phase. This discrepancy originates from the differences in the partial atomic charges used in previous calculations and the present work (using CHARMM22). The calculated values for the amide frequencies as compared to the corresponding experimental values[5] are given in Table 2.

An estimate of the energy differences as a function of the (Φ,Ψ) sets can be obtained by creating a phi−psi map (Figure 1). In the present case, each dihedral angle was incremented by 30° and the total potential energy was calculated at each step; this showed that conformations near the C5 ($\Phi \approx 150°$, $\Psi \approx 180°$) and the C7 structures appear as being the lowest energy conformers as the centers of their low-energy (ϕ,ψ) range stand under 0.7 kcal mol^{-1} for both of them. Starting from the center of their lowest energy ranges, the geometries of the three hydrogen-bonded cyclic conformations, C7$_{eq}$ ($\Phi \approx -70°$, $\Psi \approx 70$), C7$_{ax}$ ($\Phi \approx 75$, $\Psi \approx -75$), and C5, have been optimized, and the C7$_{eq}$ conformer was found to be the most stable. It is noteworthy that the major contribution to the potential energy arises from the electrostatic potential.

Table 3 gives the final optimized geometrical parameters obtained from the SPASIBA/CHARMM and the CHARMM force fields.

The relative energy differences between the three conformers are compared to the ab initio and MP2 calculations of MacKerell et al.[4] A discrepancy can be noted for the relatively low empirical dipole moment calculated for the C7$_{ax}$ conformer (2.74 D) relative to the value calculated by MacKerell et al. (3.56 D).[4] We have to point out again that atomic charges given in the CHARMM22 force field were used in the hybrid SPASIBA/CHARMM force field. Inversely, the C5 conformation gives the largest dipole in the present case. It is important to note that the present calculations were done in the gas phase and that no solvent effects were taken into account.

III.c. Alkanes. The structure and vibrational properties of a series of alkanes have been previously studied.[6] The specific SPASIBA parameters and equilibrium values were determined

TABLE 2: Comparison between the Characteristic Amide Frequencies (in cm^{-1}) Obtained from the Modified SPASIBA/CHARMM (1) and Original CHARMM (2) Force Fields for the Alanyl Dipeptide $C_1H_3-C_5O-N_7H-C_9H(C_{11}H3)-C_{15}O-N_{17}H-C_{19}H_3$[a]

normal mode		exptl	C7 equatorial (1)	C7 equatorial (2)	C7 axial (1)	C7 axial (2)	C5 (1)	C5 (2)
γC5═O	Amide VI	538	508	612	521	656	519	
γC15═O			560	658	572		554	669
δC5═O	Amide IV	644	618	549	612	520	611	572
δC15═O		702	662	578	661		630	640
γN17−H	Amide V		729	837	716	755	678	833
γN7−H		760	758	887	764	833	841	884
δN17−H + νC15−N	Amide III	1272	1275	1184	1283	1244	1261	1218
δN7−H + νC5−N		1296	1287	1265	1286	1270	1286	1273
νC5−C7 + δN7−H	Amide II	1555	1574	1553	1552	1552	1552	1572
νC15−N17 + δN17−H			1571	1598	1570	1590	1556	1609
νC5═O	Amide I	1650	1663	1680	1658	1685	1654	1677
νC15═O			1666	1684	1663	1692	1662	1684

[a] The experimental frequencies were obtained from Shimanouchi, T.; Koyama, Y.; Itoh, K. *Prog. Polym. Sci. Jpn.* **1974**, *7*, 273. ν, stretching; δ, in-plane bending; γ, out-of-plane bending.

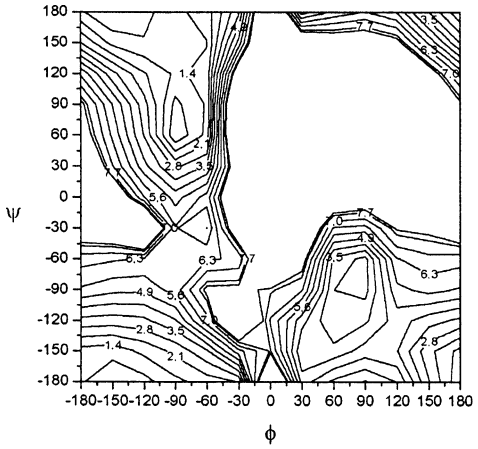

Figure 1. (ϕ,ψ) map for *N*-acetyl-L-alanine obtained from the SPASIBA force field included into CHARMM (ϕ: C′−N−CA−C′, ψ: N−CA−C′−N).

TABLE 3: Final Optimized Geometrical Parameters for L-Alanine Dipeptide as Obtained from the SPASIBA/CHARMM (1) and CHARMM (2) Force Fields

internal coordinates	C7 equatorial (1)	C7 equatorial (2)[a]	C7 axial (1)	C7 axial (2)[a]	C5 (1)	C5 (2)[a]
CT−C (ace)	1.500	1.480	1.501	1.480	1.502	1.480
C−N (ace)	1.316	1.339	1.316	1.343	1.312	1.335
C═O (ace)	1.237	1.224	1.238	1.225	1.238	1.223
N−CT	1.443	1.449	1.443	1.456	1.443	1.442
CT−C	1.496	1.529	1.498	1.527	1.497	1.517
C−N(NMe)	1.312	1.346	1.312	1.345	1.312	1.348
N−CT(NMe)	1.452	1.443	1.452	1.446	1.454	1.444
CT−C−N	117.1	116.6	117.1	115.9	117.02	116.4
C−N−CT	117.9	123.3	118.02	125.9	119.63	122.8
N−CT−C	108.5	112.6	108.4	114.9	99.45	108.2
CT−C−N	116.6	116.8	116.34	117.9	118.39	117.7
C−N−CT	118.5	122.4	118.52	122.7	117.8	121.5
ϕ(C′−N−Cα−C′)	−74.9	−81.3	72.3	69.7	−147.9	−151.4
ψ(N−Cα−C′−N)	63.8	70.6	−68.3	−67.6	−179.8	170.6
dipole (D)	2.89		2.74		3.44	
ΔE^{X-C7eq} [b]	0.		2.20		2.10	

[a] Values taken from ref 4. [b] In kcal mol^{-1}.

for methane, ethane, trans and gauche conformers of *n*-butane, neopentane, cyclohexane, *n*-octane, and *n*-decane.[7,8] The force field was checked by calculating the infrared and Raman intensities using ab initio parameters determined at the HF/6-31G*, D95* levels of theory and taking into consideration the electronic correlation through MP2 calculations.[7]

The SPASIBA force field includes the classical Urey−Bradley terms and other important terms that are essential to account for internal tension (Kappa) and angular interactions (l_{CH2}) found among valence angles around a tetrahedral atom and internal interactions between angles of adjacent methylene groups (trans and gauche interactions). These terms allow a correct fitting of the vibrational modes and explain the preferential gauche and trans conformations of *n*-alkanes. For these reasons, the SPASIBA force field is considered to be of spectroscopic quality. The correct values in energy differences between the eclipsed and staggered conformations for ethane have been shown to depend on such interactions.

Table 4 displays the calculated vibrational wavenumbers obtained after energy minimization for ethane using the SPASIBA/CHARMM force field and the corresponding normal modes using the atomic charges and nonbonded parameters given in CHARMM. The most important differences can be observed in the assignment of some symmetric bending modes of the methyl groups (1374 cm^{-1} for SPASIBA/CHARMM and 1321 cm^{-1} for CHARMM). This leads to the conclusion that internal tensions (originating from redundancy relations) around a tetrahedral atom have to be solved to correctly locate the normal modes. The calculated rms for the normal modes (10.7 cm^{-1}) in ethane using the SPASIBA/CHARMM force field is comparable to the value obtained in the previous SPASIBA calculations. The experimental data was extracted from previous work.[27] The rms obtained when using the original CHARMM22 force field has been found to be very large (>100 cm^{-1}; see Table 4) with respect to the correct normal modes assignments. As a matter of comparison, we calculated an rms of 58 cm^{-1} for the vibrational assignments of ethane[23] as given by Cornell et al. based only on three frequencies, although a force field should always be verified over all the normal modes of the molecule under consideration.

III.d. Trans *n*-Butane. The vibrational wavenumbers, determined using isotopic analogues, were used to test the accuracy of the SPASIBA force field and to reproduce experimental values such as the energy difference between the trans and cis form of *n*-butane (calculated value, 5.4 kcal mol^{-1} and experimental value 4.9 kcal mol^{-1}). Table 5 gives the calculated vibrational frequencies and potential energy distribution obtained for trans *n*-butane as calculated with the SPASIBA/CHARMM force field (rms = 20.7 cm^{-1}). A corresponding value of 8.8 cm^{-1} is obtained for the SPASIBA force field alone using its specific charges and nonbonded parameters.

TABLE 4: Ethane ($C_\alpha H_3-C_\beta H_3$) Experimental (exptl) and Calculated Vibrational Wavenumbers (cm^{-1}) for Different Force Fields[a]

exptl[b]	SPASIBA[b]	SPASIBA/CHARMM		CHARMM	
279 A2u	280	277	$1.0\tau C-C$	302	$1.0C-C$
822 Eu	823	812	$0.4\rho C_\alpha H_3 + 0.4\rho C_\beta H_3$	806	$0.46\rho C_\alpha H_3 + 0.46\rho C_\beta H_3$
	823	812		806	
995 A1g	999	995	$0.96\nu C-C$	790	$0.83\nu C-C$
1190 Eg	1188	1185	$0.42\rho C_\alpha H_3 + 0.42\rho C_\beta H_3$	973	$0.46\rho C_\alpha H_3 + 0.46\rho C_\beta H_3$
	1188	1185		973	
1370 A2u	1376	1374	$0.45\delta sC_\alpha H_3 + 0.45\delta sC_\beta H_3$	1321	$0.5\delta sC_\alpha H_3 + 0.5\delta sC_\beta H_3$
1388 A1 g	1382	1374.2	$0.49\delta sC_\alpha H_3 + 0.49\delta sC_\beta H_3$	1364	$0.46\delta aC_\alpha H_3 + 0.46\delta aC_\beta H_3$
1460 Eu	1446	1446	$0.47\delta aC_\alpha H_3 + 0.47\delta_\alpha C_\beta H_3$	1364.3	
	1446	1446		1381	$0.47\delta aC_\alpha H3 + 0.47\delta aC_\beta H3$
1469 Eg	1453	1450.2	$0.45\delta aC_\alpha H_3 + 0.45\delta aC_\beta H_3$	1381	
	1453	1450.2		1406	$0.41\delta aC_\alpha H_3 + 0.41\delta aC_\beta H_3$
2915 A2u	2895	2894	$0.5\nu sC_\alpha H_3 + 0.5\nu sC_\beta H_3$	2788	$0.5\nu sC_\alpha H_3 + 0.5\nu sC_\beta H_3$
2915 A1g	2921	2921	$0.49\nu sC_\alpha H_3 + 0.49\nu sC_\beta H_3$	2796	$0.5\nu sC_\alpha H_3 + 0.5\nu sC_\beta H_3$
2950 Eg	2962	2961	$0.49\nu aC_\alpha H_3 + 0.49\nu aC_\beta H_3$	2896	$0.5\nu aC_\alpha H_3 + 0.5\nu aC_\beta H_3$
	2962	2961		2896	
2974 Eu	2977	2976	$0.5\nu aC_\alpha H_3 + 0.5\nu aC_\beta H_3$	2901	$0.5\nu aC_\alpha H_3 + 0.5\nu a\ C_\beta H_3$
	2977	2976		2901	
$\lvert\Delta\nu\rvert$ (cm^{-1})	7.5	9.0		78.1	
rms (cm^{-1})	9.3	10.7		114.4	

[a] ν, stretching; νs and νa, symmetric and antisymmetric stretchings; τ, torsion; $\Delta\nu$, mean deviation; δ and ρ, in-plane bending and rocking deformations; δs and δa, symmetric and antisymmetric deformations. [b] Calcd; see ref 12.

TABLE 5: Calculated Vibrational Frequencies (in cm^{-1}) of Trans *n*-Butane $C_1H_3-C_2H_2-C_3H_2-C_4H_3$ as Obtained from the SPASIBA (1) and SPASIBA/CHARMM (2) Force Fields[a]

exptl[6]	(1)	(2)		exptl[6]	(1)	(2)	
121	118	113	τC_2-C_3	1378	1383	1370	$\delta sC_1H3 + \delta sC_4H3$
	224	204	$\tau C_1-C_2 + \tau C_3-C_4$	1441	1432	1434	$sciC_2H2 + sciC_3H2$
	257	239	$\tau C_1-C_2 + \tau\ C_3-C_4$	1441	1434	1440	$sciC_2H2 + sciC_3H2$
323	303	280	$\delta C_1C_2C_3 + \delta C_2C_3C_4$	1451	1452	1451	$\delta aC_1H3 + \delta aC_4H3$
421	415	391	$\delta CCC + \nu C-C$	1455	1455	1451	$\delta aC_1H3 + \delta aC_4H3$
732	715	690	$\rho C_2H2 + \rho C_3H2$	1459	1455	1452	$\delta aC_1H3 + \delta aC_4H3$
829	807	777	$\rho C_2H2 + \rho C_3H2$	1468	1458	1455	$\delta aC_1H3 + \delta aC_4H3$
	856	851	$\nu C_2-C_3 + \rho CH3$		2851	2850	$\nu sC_2H2 + \nu sC_3H2$
964	976	956	$\rho CH3$		2871	2872	$\nu sC_2H2 + \nu sC_3H2$
979	979	967	$\rho CH3$		2886	2887	$\nu aC_2H2 + \nu aC_3H2$
1009	1005	997	$\nu C_1-C_2 + \nu C_3-C_4$		2900	2900	$\nu aC_2H2 + \nu aC_3H2$
	1039	1023	$\nu C_1-C_2 + \nu C_2-C_3 + \nu C_3-C_4$		2910	2910	$\nu sC_1H3 + \nu s\ C_4H3$
1132	1122	1132	$\nu C_2\_C_3 + \rho CH_3 + \delta\ CCC$		2911	2911	$\nu sC_1H3 + \nu sC_4H3$
1168	1174	1167	$\rho CH3$		2969	2968	$\nu aC_1H3 + \nu a\ C_4H3$
1258	1261	1265	$twC_2H2 + twC_3H2$		2969	2969	$\nu aC_1H3 + \nu a\ C_4H3$
1291	1290	1270	$twC_3H2 + twC_2H2$		2970	2969	$\nu aC_1H3 + \nu a\ C_4H3$
1338	1321	1307	$wagC_2H2 + wagC_3H2$		2970	2969	$\nu aC_1H3 + \nu a\ C_4H3$
1343	1335	1330	$wagC_2H2 + wagC_3H2 + \nu C_2-C_3$				
1377	1382	1368	$\delta sC1H3 + \delta sC4H3$	rms	8.8	20.7	

[a] rms, root-mean-square (in cm^{-1}); ν, stretching; δ, in-plane bending; δs and δa, symmetric and antisymmetric in-plane bending; sci, scissor; wag, wagging; tw, twisting; ρ, rocking; τ, torsion.

III.e. Methylethyl Ether. The ether functional group has been previously studied.[9] The structural parameters for methylethyl ether were obtained from electron diffraction[28] and microwave studies.[29] The experimental vibrational wavenumbers were obtained by Perchard.[30] For this molecule, three conformers (gauche, cis, and trans) have been shown to exist, the most stable one being the trans conformer with an energy difference of 1.4 kcal mol^{-1} relative to the gauche conformer. In the work of Tristram et al.,[9] deuterium substitutions were used to determine a correct parametrization for the ether function group in the SPASIBA force field. These authors found a trans-to-gauche ΔE^{T-G} energy difference of 1.51 kcal mol^{-1}; a value of 1.38 kcal mol^{-1} was obtained using the SPASIBA/CHARMM force field. A dipole moment of 1.57 D was calculated using the SPASIBA force field (a value of 1.98 D was determined from HF/6-31G* ab initio studies). A topology file for methylethyl ether (MAS) has been created, and the corresponding SPASIBA parameters have been added to the SPASIBA/CHARMM parameter set.

Table 6 gives the vibrational wavenumbers and potential energy distribution obtained from the SPASIBA/CHARMM force field. An rms of 18 cm^{-1} relative to the experimental data was found.

The final optimized geometric values for the CC, CO, CCO, and COC parameters agree in a satisfactory way with the values obtained by Tristram et al.,[9] however, a lower dipole moment was obtained (1.51 D for SPASIBA/CHARMM versus 1.73 D for SPASIBA calculations). This discrepancy could arise again from the different atomic charges and van der Waals parameters used in the two force fields.

III.f. Ethanethiol (C_2H_5SH). For ethanethiol, three molecular conformations can be put in evidence with staggered conformations about the C−S bond (two gauche enantiomers g+, g− with C_1 group symmetry and one trans conformer t with C_s

TABLE 6: Vibrational Frequencies (in cm^{-1}) for Methylethyl Ether (Me−O−Et)[a]

exptl[30]	SPASIBA[9]		SPASIBA/CHARMM
	130	124	$0.96\tau C_{Et}-O$
	209	216	$0.96\tau C_{Me}-O$
	250	397?	$0.96\tau C-C$
	291	301	$0.34\delta OCC$
	424	428	$0.42\delta COC + 0.22\delta OCC$
800	816	768	$0.52\rho CH3_{Et}$
844	849	847	$0.40\nu O-C_{Et} + 0.3\rho CH3_{Et}$
984	1008	1038	$0.31\nu C_{Et}O + 0.23\nu C_{Me}O + 0.08\delta OCH$
1071	1037	1090	$0.71\nu C_{Me}-O + 0.16\nu O-C_{Et}$
1134	1157	1112	$0.18\rho CH2 + 0.14\rho CH3_{Et} + \rho CH3_{Me}$
1175	1159	1162	$0.74\rho CH3_{Me}$
		1167	$0.56\nu C-C$
1217	1212	1214	$0.55\rho CH3_{Me} + 0.3\nu C_{Et}O$
1276	1283	1293	$0.70\delta CH3_{Et} + 0.17\delta CH2$
1310	1330	1310	0.74twCH2
1396	1396	1380	$0.52\nu(C-C)_{Et} + 0.2\delta CH2 + 0.16\delta sCH3_{Et}$
1448	1454	1448	0.83wagCH2
	1454	1453	$0.82\delta aCH3_{Et}$
1456	1463	1459	0.67sciCH2
	1464	1463	$0.92\delta aCH3_{Me}$
	1476	1474	$0.93\delta aCH3_{Me}$
	1495	1495	0.67sciCH2
	2816	2815	$0.98\nu sCH3_{Et}$
2867	2866	2887	$1.0\nu sCH3_{Et}$
2907	2923	2947	$1.0\nu aCH3_{Et}$
2933	2925	2948	$1.0\nu aCH3_{Et}$
	2964	2963	$1.0\nu aCH3_{Me}$
	2992	2991	$1.0\nu sCH2$
	2996	2995	$1.0\nu aCH3_{Me}$
	3023	3022	$1.0\nu aCH2$
rms	15	18	

[a] ν, stretching; δ, in-plane bending; δs and δa, symmetric and anti symmetric deformations; sci, scissor; wag, wagging; tw, twisting methylene deformations; ρ, rocking; rms, root-mean-square deviation (in cm^{-1}).

symmetry. At room temperature, the infrared spectra cannot differentiate between the three conformers.[31] Infrared and normal mode analysis were performed[31] in order to evaluate the relative contributions of the gauche and trans conformers. The ethanethiol molecule was studied in different physical states (gas, liquid, and crystal states). With the use of calorimetric data and infrared experiments, it was found that the C_1 conformer (g and g′) is more stable by 0.2−0.3 kcal mol^{-1} with respect to the trans one. Table 7 shows the calculated vibrational wavenumbers and potential energy distribution among the internal coordinates (given for the gauche conformer) both for the original SPASIBA (rms = 7 cm^{-1}) and for SPASIBA/CHARMM force fields. In the present work, the electrostatic potential was calculated using atomic charges derived from quantum chemical calculations (density functional theory, DFT) using the B3LYP functional and a 6-31G** basis set.

Molecular dynamics studies under the pure SPASIBA force field were performed in the present work for ethanethiol in the gas phase at 300 K to study the relative proportions of the g+, g−, and t conformers versus time.

The relative population of a given conformer is displayed in Table 8 (starting from a gauche g+ conformer). After 70 ps of simulation, the g+ conformer proportion decreases from 1.00 to 0.22 while the g− conformer appears to an extent of 0.78. From 90 to 150 ps, the g conformers become the predominant form until the appearance of the three conformers in equal proportions after 500 ps according to the experiments. When CHARMM is used, the percentage of the trans conformer reaches only 10%. The energy difference between the g+ or g− and t conformers was calculated to be 0.2 kcal mol^{-1}, this value being of the same order as the experimental value obtained from calorimetric data. This result shows clearly that such a small difference in energy would lead to the appearance of equal relative amounts of each conformer and to the predominance of the gauche forms. Effectively, after 500 ps of dynamics, the g+, g−, and t conformers are of equal probability. When the original CHARMM parameter set is used, the proportions are 0.56, 0.1, and 0.34 for the g+, t, and g− conformers, respectively.

III.g. Methyl Acetate. Esters form an another important class of molecules for which molecular mechanics studies can be performed to investigate the effect of their insertion into esters groups of glycolipids.

TABLE 7: Experimental (exptl) and Calculated Vibrational Wavenumbers (cm^{-1}), and Potential Energy Distribution for Ethanethiol (CH_3-CH_2-SH) [a]

exptl[21]		SPASIBA		SPASIBA/CHARMM
191	191	$\tau_{C-S}(0.99)$	202	$\tau_{C-S}(0.97)$
246	251	$\tau_{C-C}(0.99)$	245	$\tau_{C-C}(0.98)$
331	335	$\delta_{CCS}(0.54)$, $\nu_{C-S}(0.27)$, $\nu_{CC}(0.07)$	319	$\delta_{CCS}(0.78)$, $\nu_{C-S}(0.11)$, $\nu_{C-C}(0.04)$
658	653	$\nu_{C-S}(0.82)$, $\delta_{CCS}(0.05)$, $\delta_{CSH}(0.03)$	636	$\nu_{C-S}(0.66)$, $\delta_{CSH}(0.17)$, $\delta_{CCS}(0.07)$
738	742	$\rho_{CH2}(0.45)$, $\nu_{C-C}(0.19)$, $\rho_{CH3}(0.17)$	796	$\rho_{CH2}(0.70)$, $\rho_{CH3}(0.12)$
871	872	$\delta_{CSH}(0.57)$, $\nu_{CC}(0.25)$, $\nu_{C-S}(0.14)$	766	$\delta_{CSH}(0.80)$, $\nu_{C-S}(0.15)$
971	980	$\nu_{C-C}(0.64)$, $\delta_{CSH}(0.14)$, $\delta_{CCH}(0.05)$	986	$\rho_{CH3}(0.37)$, $\nu_{C-C}(0.38)$, $\rho_{CH2}(0.07)$
1051	1052	$\rho_{CH3}(0.28)$, $\nu_{CC}(0.18)$, $\rho_{CH2}(0.12)$	1026	$\rho_{CH3}(0.71)$, $\rho_{CH2}(0.21)$
1092	1057	$\rho_{CH3}(0.56)$, $\rho_{CH2}(0.28)$, $\tau_{C-C}(0.10)$	1040	$\rho_{CH3}(0.46)$, $\nu_{CC}(0.36)$, $\delta_{CCS}(0.06)$
1253	1255	$tw_{C2H2}(0.61)$, $\delta_{CH3}(0.12)$, $\nu_{C-S}(0.07)$	1196	$tw_{CH2}(0.94)$
1274	1277	wag $_{C2H2}(0.6)$, $\delta_{CH3}(0.33)$	1374	$wag_{CH2}(0.82)$, $\nu_{C-C}(0.09)$
1379	1371	$\delta s_{CH3}(0.95)$, $\nu_{C-C}(0.03)$	1413	$\delta s_{CH3}(0.90)$, $\nu_{C-C}(0.09)$
1431	1433	$sci_{C2H2}(0.82)$	1447	$sci_{CH2}(0.85)$
1449	1454	$\delta a_{CH3}(0.91)$	1422	$\delta a_{CH3}(0.82)$
1457	1457	$\delta a_{CH3}(0.94)$	1428	$\delta a_{CH3}(0.95)$
2571	2575	$\nu_{S-H}(1.0)$	2575	$\nu_{S-H}(1.0)$
2875	2879	νsCH2(0.84)	2851	$\nu s_{CH2}(0.99)$
2902	2909	νsCH3(0.87)	2882	$\nu a_{CH2}(0.99)$
2928	2916	νaCH2(0.98)	2902	$\nu s_{CH3}(0.99)$
2967	2970	νa CH3(0.99)	2958	$\nu a_{CH3}(1.0)$
2980	2971	νa CH3(1.0)	2959	$\nu a_{CH3}(1.0)$
m	1.45		1.45	
rms	7.3		19.1	

[a] ν, stretching; δ, in-plane bending; τ, torsion; sci, scissor; wag, wagging; tw, twisting; ρ, rocking. μ, calculated dipole moment (in Debye); rms, root-mean-square deviation (in cm^{-1}).

TABLE 8: Ethanethiol Dihedral Percent of Gauche and Trans Conformers vs Time (ps)[a]

	SPASIBA Percentage of conformers after (ps)										CHARMM percentage
time (ps)	50	60	70	80	90	100	150	200	250	500	after 500ps
Gauche+	100	100	22	29.5	23	81	100	70	31	33	56
Trans			0	0	0	0	0	11.5	37	34	10
Gauche−			78	70.5	77	19	0	18.5	32	33	34

[a] The atomic charges were derived from DFT (B3LYP/6-31G** quantum calculations. C(CH3) −0.326, H(CH3) 0.1153, 0.1165, 0.1327, C(CH2) −0.318, H(CH2) 0.1464, 0.1431, S −0.081, H(SH) 0.072.

Chhiba et al.[10] determined the associated SPASIBA force field parameters for several molecules taken as models (methyl formate and ethyl formate, methyl acetate) and compared the calculated dipole moments and moments of inertia to their related experimental values. In the present work, we transferred directly the SPASIBA force field parameters for bonds, valence angles, and torsional angles. The CHARMM program was modified to accept *n*-fold terms for improper torsions, and we used those values given by Chhiba et al. ($n = 2$, 2-fold rotational barrier). A topology file (OET) was created and the associated SPASIBA force constants were included into the specific parameter file. Methyl acetate has a hindered rotation around the O═C−O bond, and experiments have shown that the most stable form is obtained for the planar trans structure (with an energy difference of 8.5 kcal mol^{-1} relative to the cis conformer).[32] In their work, Chhiba et al.[10] used atomic charges derived from DFT methods (Becke3LYP/6-31G*); however, in the present work, we kept the values given in the CHARMM22 library. Table 9 displays the vibrational wavenumbers and potential energy distribution deduced from the SPASIBA/CHARMM force field and, as a matter of comparison, those derived from application of the original CHARMM22 force field. The optimized geometries obtained in this work are quite comparable to those reported by Chhiba et al., with a theoretical value of 1.45 D for the dipole moment (1.68 D for the pure SPASIBA force field). Examination of the various atomic charges used for each specific force field can explain easily the differences obtained for the two kinds of calculations; however, the relative rms shows a good transferability for the SPASIBA force field.

III.h. Propene. Alkenes have been investigated as models with the perspective to apply their parameters to biological compounds such as phospholipids. Chhiba and Vergoten[11] obtained the SPASIBA parameters for a series of compounds such as ethylene, propene, isobutene, butene, butadiene, isoprene, hexatriene, and octatetraene. These authors used several deuterated species to assign correctly the normal modes for both the in-plane and out-of-plane motions. The propene molecule was chosen here to test the implementation of the SPASIBA/CHARMM and to check the transferability of alkene parameters. Table 10 displays the calculated frequencies and the PED for the original SPASIBA (AM1 charges) and for the SPASIBA/CHARMM force fields using its specific atomic charges (CHARMM22).

The experimental vibrational wavenumbers are derived from Barnes and Howells[33] A value of 2.11 kcal mol^{-1} was obtained for the methyl rotational barrier of propene. This value has to be compared to the experimental data (1.98 kcal mol^{-1}) obtained from microwave experiments.[34]

III.i. Methanol. Methanol is the simplest molecule in the series of aliphatic alcohols. Its geometry has been determined from electron diffraction studies[35] and from microwave spectroscopy.[36] However, the experimental data used to derive the force field parameters were obtained from the gas phase.[37] The vibrational frequencies and potential energy distribution for the

TABLE 9: Experimental (exptl) and Calculated Wavenumbers (cm^{-1}) for Methyl Acetate and PED for Pure SPASIBA (1), CHARMM/SPASIBA (2), and CHARMM (3) Force Fields[a]

exptl[22]	(1)[22]	(2)	PED	(3)	PED
110	117	100	τ_{C-CH3}	28?	
136	137	109	τ_{C-CH3}	96	$\tau_{C-O} + \gamma_{C=O}$
187	184	184	τ_{C-O}	221	ρ_{CH3}e
303	312	303	$\delta_{COC} + \delta_{OCO}$	188	δ_{COC}
429	432	418	$\delta_{CCO} + \delta_{OCO}$	361	$\delta_{CC-O} + \delta_{CC=O}$
607	604	610	$\gamma_{C=O}$	566	$\gamma_{C=O}$
639	625	628	$\nu_{C-C} + \delta_{OCO}$	495	$\nu_{C-C} + \delta_{OCO} + \delta_{CCO} + \nu_{C-O}$
844	849	846	$\nu_{C-O} + \nu_{C=O} + \delta_{COC}$	598	$\nu_{C-O} + \nu$C−C + r_{CH3}
980	993	983	ρ_{CH3}ac + $\nu_{C-O} + \nu_{C=O}$	871	ρ_{CH3}ac + $\gamma_{C=O}$
1036	1060	1058	ρ_{CH3}ac + $\gamma_{C=O}$	1103	δ_{CH3}e
1060	1096	1097	$\nu_{C-O} + \nu_{C-CH3}$	980	ν_{O-CH3}e + $\delta_{CCO} + \rho_{CH3}$
1159	1158	1149	ρ_{CH3}e	1114	ρ_{CH3}ac + ρ_{CH3}e + $\nu_{C-O} + \delta_{CCO} + \delta_{OCO}$
1187	1169	1171	ρ_{CH3}e + $\delta_{COC} + \nu_{C=O} + \nu_{C-O}$	1135	ρ_{CH3}e
1248	1278	1262	ρ_{CH3}ac + $\nu_{C-O} + \nu_{C-CH3}$	1285	ρ_{CH3}ac + ν_{C-C}
1375	1357	1348	δs_{CH3}ac + γ_{C-O}	?	
1430	1454	1439	δs_{CH3}e	1365	δ_{CH3}ac
1430	1457	1452	δa_{CH3}ac	1366	δ_{CH3}ac
1440	1459	1454	δa_{CH3}ac	1415	δa_{CH3}e
1460	1478	1471	δa_{CH3}e	1417	δs_{CH3}e
1460	1479	1476	δa_{CH3}e	1545	δa_{CH3}e
1771	1776	1770	$\nu_{C=O}$	1722	νC═O
2964	2940	2944	$\nu s_{C-H}(CH_3ac)$	2787	$\nu s_{C-H}(CH_3ac)$
2966	2945	2964	$\nu s_{C-H}(CH_3e)$	2793	$\nu s_{C-H}(CH_3e)$
2994	3003	3004	$\nu a_{C-H}(CH_3ac)$	2899	$\nu a_{C-H}(CH_3ac)$
3005	3006	3006	$\nu a_{C-H}(CH_3ac)$	2901	$\nu a_{C-H}(CH_3ac)$
3031	3008	3021	$\nu a_{C-H}(CH_3e)$	2902	$\nu a_{C-H}(CH_3e)$
3035	3027	3023	$\nu a_{C-H}(CH_3e)$	2905	$\nu a_{C-H}(CH_3e)$
rms	15.4 cm^{-1}	15.08		104.6	

[a] ac, acetate; e, ester; ν, stretching; νs and νa, symmetric and antisymmetric stretching; δ, in-plane bending; δs and δd, symmetric and antisymmetric in-plane deformations; ρ, rocking deformation; γ, out-of-plane deformation; τ, torsion; rms, root-mean-square deviation (in cm^{-1}).

TABLE 10: Propene Experimental and Calculated Wavenumbers (cm^{-1}) and Associated PED as Obtained from SPASIBA (1) and SPASIBA/CHARMM (2) Force Fields[a]

exptl[24]	(1)[24]	(2)	
174	189	185	τC−C
428	427	421	06δC−C=C + 0.2δC−H
578	574	587	0.8τC=C + τC−C
912	896	884	0.95wagCH2
920	918	933	0.62νC−C + 0.11νC−C
935	931	940	0.75rCH2
991	997	984	0.5rCH3 + 0.17rCH2
1045	1044	1040	0.79wagCH2 + δCH3
1172	1166	1190	0.45rCH2 + 0.31νC−C
1298	1302	1306	0.4δC−H + 0.14νC=C + 0.14rCH2
1378	1388	1366	0.82δsCH3 + 0.07νC=C + 0.06νC−C
1419	1426	1431	0.78δCH2
1443	1446	1448	0.84δCH3
1474	1454	1451	0.85δCH3
1652	1645	1643	0.79νC=C + 0.06νC−C
2932	2937	2948	1.0νsCH3
2953	2987	2997	0.81νsCH2
2973	2991	3004	0.82νaCH(CH3) + 0.13νCH(CH2)
2991	2995	3006	1.0νaCH(CH3)
3017	3010	3033	0.82νCH (C−H)
3091	3091	3089	0.99νsCH2

[a] ν, stretching; δ, bending; r, rocking; a and s, antisymmetric and symmetric motions; τ, torsion.

SPASIBA force field and SPASIBA/CHARMM are given into Table 11.

The rms for wavenumbers are quite comparable and in agreement with the value obtained by Tristram et al.[12] In the present work, the nonbonded parameters and atomic charges were taken from the CHARMM22 library. The dipole moment and optimized geometries obtained from SPASIBA/CHARMM are in quite good accordance with the experimental data, but the torsional barrier for the Me−C bond is, however, calculated with a lower value (0.85 kcal mol^{-1}) than for the experimental one (1.07 kcal mol^{-1}). The calculated dipole moment (1.94 D) is of the same order of magnitude as the values obtained from ab initio methods.

III.j. Ethanol. For ethanol, Schaefer[38] has shown that the trans form is more stable than the gauche form by about 0.46 kcal mol^{-1}. Tristram et al.[12] calculated the SPASIBA parameters for trans ethanol and found a difference of 0.3 kcal mol^{-1} between the two conformers and a C−C rotational barrier of 2.95 kcal mol^{-1} (3.08 experimentally). They obtained a calculated value of 2.5 D for the dipole moment. In the present work, ab initio charges obtained from HF/6-31G* calculations lead to a calculated dipole moment of 1.92 D for trans ethanol. A dipole moment of 2.34 D is therefore calculated using the atomic charges given in the CHARMM library.

Table 12 displays the calculated vibrational wavenumbers and potential energy distribution using SPASIBA/CHARMM. The optimized geometry parameters are in good agreement with the experimental values, that is, C−C = 1.54 Å (1.529 Å), C−O = 1.42 Å (1.425 Å), O−H = 0.950 Å (0.945 Å) for bonds and C−C−O = 109.4° (108°) and C−O−H = 107.5° (108°) for the valence angles with the experimental values given in parentheses.

For SPASIBA/CHARMM, the calculated energy difference between the trans and gauche forms appears herein to be slightly overestimated (−0.69 kcal mol^{-1}) but the C−C torsional barrier value remains in quite good agreement (3.06 kcal mol^{-1}) with the experiments. The calculated rms values are 15.4, 24.9, and 44.1 cm^{-1} as obtained from the SPASIBA, SPASIBA/CHARMM, and original CHARMM force fields, respectively. The most important deviations appearing in the calculated normal modes are related to the methylene and methyl deformations. The wavenumbers obtained for the SPASIBA force field show explicitly that the F, F', Kappa, and l_{CH2} terms are essential to correctly locate the rocking, twisting, wagging, and scissoring motions of the methylene and the symmetric and antisymmetric deformations of the methyl groups.

III.k. α- and *β*-D-Glucose. The vibrational force field for α- and β-D-glucose in the crystal state was first investigated in our group by Dauchez et al.[13] The orientation of the anomeric OH group is axial in the α and equatorial in the β anomers. Both anomers have a C_1 symmetry group and crystallize in the orthorombic system ($P2_12_12_1$ space group). Dauchez et al. used Raman and infrared vibrational spectroscopies to determinate the SPASIBA parameters using deuterated analogues to check for specific assignments particularly between 600 and 1000 cm^{-1}. This force field was recently taken as a starting point for molecular mechanics studies for both α- and β-D-glucose anomers[2] and disaccharides with different glycosidic linkages. The 600−1000 cm^{-1} range can be divided into the fingerprint and crystalline regions. Raman bands observed at 916, 842, and 773 cm^{-1} are specific of the α-D-glucose anomer. The 842 cm^{-1} band involves methylene deformation modes and all the stretching vibrations arising from the hemiacetal group $C_5-O_5-C_1-O_1$. The 773 cm^{-1} band contains in-plane COC and CCC deformations and endo and exocyclic C_1-O stretching modes. The corresponding modes are calculated with SPASIBA/CHARMM at 912, 843, and 747 cm^{-1}, respectively, and their

TABLE 11: Methanol Experimental (exptl) and Calculated Vibrational Frequencies (in cm^{-1}) and Potential Energy Distribution as Obtained from CHARMM and SPASIBA Force Fields[a]

exptl[30]	SPASIBA		CHARMM		SPASIBA/CHARMM	
271	268	1.0τCO	263	1.0τCO	276	1.0τCO
1033	1032	0.75rCH3 + 0.25δCOH	962	0.9rCH3 + δCOH	1029	0.6rCH3 + 0.36δCOH
1076	1077	0.94νCO	1026	0.62νCO + 0.35rCH3	1077	0.94νCO
1145	1132	0.9rCH3 + δ OCH3	987	0.99rCH3	1132	0.92rCH3
1334	1332	0.61δCOH + 0.3rCH3	1321	0.81δCOH	1329	0.55δCOH + 0.37rCH3
1451	1460	0.85δsCH3	1377	0.95δCH3	1461	0.92δsCH3
1466	1466	0.94δdCH3	1378	0.99δCH3	1462	0.97δaCH3
1473	1476	0.96δdCH3	1502	0.66δCH3 + 0.32νCO	1475	0.95δaCH3
2844	2845	0.97νsCH3	2735	1.0νsCH3	2845	0.97νsCH3
2960	2965	0.96νaCH3	2841	1.0νaCH3	2965	1.0νaCH3
3000	2992	0.99νaCH3	2842	1.0νaCH3	2992	1.0νaCH3
3681	3691	1.0νOH	3682	1.0νOH	3684	1.0νOH
	$\lvert\Delta\nu\rvert$ = 4.7 cm^{-1}		$\lvert\Delta\nu\rvert$ = 73.1 cm^{-1}		$\lvert\Delta\nu\rvert$ = 5.08 cm^{-1}	
	rms = 5.8 cm^{-1}		rms = 76.1 cm^{-1}		rms = 5.7 cm^{-1}	

[a] ν, stretching; s and a, symmetric and antisymmetric modes; δ, in-plane bending deformation; τ, torsion; $\Delta\nu$, standard deviation; rms, root-mean-square deviation.

TABLE 12: Ethanol Experimental (exptl) and Calculated Vibrational Wavenumbers (cm^{-1}) and Potential Energy Distribution Expressed as a Function of the SPASIBA (1), SPASIBA/CHARMM (2), and CHARMM (3) Force Fields[a]

exptl[30]	(1)[30]	(2)	PED	(3)	PED
	230	241	1.0τC−O	244	1.0τC−O
	244	292	0.98τC−C	295	0.95τC−C
419	404	408	0.67δC−O + 0.05νC−O	409	0.74δCCO + 0.1τC−C + 0.03τC−O
800	772	789	0.3rCH$_3$ + 0.29rCH$_2$ + 0.24τC−C	760	0.46rCH$_2$ + 0.32rCH$_3$ + 0.16τC−C
879	856	856	0.6νC−O + 0.12rCH$_3$ + 0.09νC−C	773	0.57νC−C + 0.23rCH$_3$ + 0.04δCCO
1030	1020	1012	0.68νC−C + 0.1δCOH + 0.06rCH$_3$	878	0.62rCH$_3$ + 0.13νC−C + 0.07νC−O
1066	1088	1055	0.57νC−O + 0.14rCH$_3$ + 0.1νC−C	934	0.55rCH$_3$ + 0.27rCH$_2$ + 0.07τC−C
1090	1113	1135	0.38rCH$_3$ + 0.3rCH$_2$ + 0.2τC−C	1013	0.39νC−O + 0.35rCH$_2$
1241	1243	1239	0.65δCOH + 0.1twCH$_2$ + 0.1ν C−O	1137	0.87twCH$_2$
	1337	1351	0.65wagCH$_2$	1295	0.6δCH$_3$ + 0.3twCH$_2$
1370	1369	1352	0.82δsCH$_3$ + 0.11wagCH$_2$	1325	0.83wagCH$_2$ + 0.1νC−O
1390	1375	1357	0.44wagCH$_2$ + 0.22δCOH	1395	0.35δCH$_3$ + 0.32wagCH$_2$ + 0.18νC−C
1445	1449	1461	0.91δaCH$_3$	1404	0.84δCH$_3$
1445	1449	1463	0.80δaCH$_3$	1406	0.84δCH$_3$
1480	1490	1498	0.65sciCH$_2$ + 0.1δCOH	1510	0.57sciCH$_2$ + 0.26νC−O
	2791	2789	0.99νsCH$_3$	2792	1.0νsCH$_3$
2984	2884	2883	1.0νaCH$_3$	2899	0.99νaCH$_3$
2928	2914	2913	1.0νaCH$_3$	2900	0.99νaCH$_3$
	2943	2959	0.98νsCH$_2$	2774	0.97νsCH$_2$
2975	2971	2990	0.98νaCH$_2$	2840	1.0 ν CH$_2$
	3690	3683	1.0νO−H	3683	1.0νO−H
$\lvert\Delta\nu\rvert$	13.1	20.2		37.4	
rms	15.4	24.9		44.1	

[a] ν, stretching; δ, bending in-plane; τ, torsion; r, rocking; wag, wagging; sci, scissor; a and s, antisymmetric and symmetric motions; $|\Delta\nu|$ and rms, mean deviation and root-mean-square (in cm^{-1}).

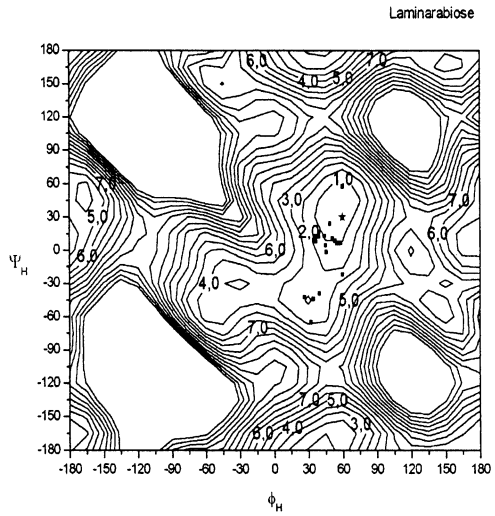

Figure 2. $\Phi_H-\Psi_H$ map for laminarabiose **(***O*-(β-D-glucopyranosyl)-(1→3)-β-D-glucopyranose). Square dots represent the energy minima obtained from known crystal structures while the star gives the calculated global minimum obtained from the SPASIBA/CHARMM force field.

corresponding assignments are given in Table 13. For the β anomer, the bands observed at 917 and 740 cm^{-1} are calculated at 950 and 763 cm^{-1} using different values for the C−C and C−O stretching modes.[39] Examination of the potential energy distribution given in Table 13 shows correct assignments for both conformers.

III.l. A Disaccharide: Laminarabiose. Laminarabiose (β-D-glucopyranose,1-3, β-D-glucopyranose) is a reducing disaccharide having generally no internal stabilizing hydrogen bonds. A phi−psi map was performed to establish the global and local minima that could appear for this disaccharide using the SPASIBA torsional potential[39] for the glycosidic linkage. The dielectric constant was set to 3.5 to mimic an apolar medium. In the Φ_H,Ψ_H map (Figure 2), several minima can be found for different sets, that is, (−40°,−30°), (−40°,180°) and neighboring local minima at (170°,−40°) and (180°,0°). Some of these values correspond quite well to the (Φ_H,Ψ_H) values obtained by Kitamura et al.[40] from Monte Carlo studies on (1→3) β-D glucans in solution.

In the present work, more minima can be predicted when using the SPASIBA force field. The predicted Φ_H,Ψ_H minima obtained here are also in accordance with the values obtained from HF/6-31G* ab initio studies by French et al.[41] These authors determined the energy surface for several different disaccharides (in the crystal state) by mixing ab initio quantum mechanics (QM) and molecular mechanics (MM). However, for laminarabiose (and nigerose) they could obtain only one local minimum, although many others are predicted in this case. This fact must be related to the higher potential flexibility given by the SPASIBA force field.

IV. Other Classes of Molecules

Other important classes of molecules have been investigated in our group that have not been discussed here. A series of aliphatic acids (acetic, pivalic, succinic, adipic, and L-glutamic) was studied by Chhiba et al.[14] and the SPASIBA spectroscopic potential was determined. The related hydrogen bond parameters between dimers have been determined. A rms of 13−15 cm^{-1} was calculated for the whole class of aliphatic acids.

Model compounds related to lipids of biomembranes have also been investigated by our group by taking into account molecules such as alkyl phosphates, acetylcholine, choline, and dimethyl phosphate anion,[15] and their related SPASIBA parameters, structures, and conformational energy differences have also been determined. Vibrational wavenumbers and assignments were checked using deuterated analogues. These parameters have been used for dynamical simulations of biomembranes taking into account hydration shells around hydrophilic groups.[16] More recently, a SPASIBA force field for aldehydes (methanal, ethanal, propenal, ethanedial, propenal, and 2-methylpropenal) has been determined by Zanoun et al.[17]and Durier

TABLE 13: α- and β-Glucose Vibrational Frequencies (in cm^{-1}) as Obtained from the SPASIBA/CHARMM[a]

ν_{exptl} (cm^{-1})	α-glucose	ν_{exptl} (cm^{-1})	β-glucose	PED (α-glucose)
86	74		73	τ_{O-C}, τ_{C-C}
112	99		108	τ_{O-C}, $_{C-C}$
135	121	158	123	τ_{O-C}, τ_{C-C}
180	161	169	175	τ_{O4-C4}(0.55), τ_{O-C}
210	171	185	211	τ_{O5-C5}(0.1), δ_{CC6O}
232	238		286	τ_{O-C}(0.36), δ_{CCO}
255	254	247	294	τ_{O2-C2}(0.45) + δ_{CCO}
271	294	273	308	τ_{O2-C2}(0.24), δ_{CCO}
289	304	288	317	δC_{C6O}, δ_{CC5C}(0.15), τ_{C6-O}(0.15)
309	321	321	331	δ_{OC3C}(0.17), (δ_{CC3O},δ_{OC3C})(0.22), τ_{C3O}
347	354	350	343	δ_{OC1O}, δ_{C1OH}, τ_{C-O}
366	369		381	δ_{O1C1O5}, ν_{C1O1}, δ_{C1O1H}, $\tau_{C1-O}1$
396	390		398	δ_{CCC}, δ_{CCO}(0.2), τ_{C6-O}
408	394	404	405	τ_{C6-O}, τ_{C2-O}, δ_{CCO}
425	410	427	417	δ_{CCO}(0.27), ν_{C-O}(0.20)
440	452	457	452	τ_{C3-O}
496	473	522	475	δ_{CCO}, ν_{C-O}, τ_{C6-O}
543	491	530	506	τ_{C3-O}
556	535	577	555	ν_{C-O}(0.25), δ_{OCO}, δ_{CCO}(0.13)
581	552	583	573	δ_{OC1O}(0.14), δ_{CCO}(0.25), ν_{C-O}(0.12)
614	601	607	597	δ_{OC1C}, δ_{CCO}(0.43), ν_{C-O},$_{C5-O}$(0.11)
649	623	634	644	δ_{OCO}, δ_{CC1O}, δ_{CC4O}(0.24)
774	747	677	654	ν_{C-O}, ν_{C-C}(0.54), δ_{COC}(0.10)
840	843	740	763	δ_{CCH}(0.27), δ_{OCH}(0.27), $\nu_{C-O,C-C}$(0.33)
914	912	917	950	ν_{C1-C2},$_{C2-C3}$(0.29), ν_{C-O}(0.13), δ_{CO5C}, δ_{CCO}, δ_{COH}(0.27)
993	982	980	983	ν_{C-C}(0.25), ν_{C-O}(0.22), δ_{COH}(0.11)
1003	989	1011	997	ν_{C-O}(0.31), ν_{C-C}(0.32)
1024	1034	1032	1018	ν_{C1-O5}(0.45), δ_{C1OH}(0.29), ν_{C-O}(0.07)
1050	1056	1052	1031	ν_{C4-C5}(0.42), ν_{CC}(0.20)
1069	1070	1068	1059	ν_{C6-O}(0.69), ν_{C-O}(0.14)
1077	1096	1081	1085	ν_{C2-O}(0.2), ν_{C4-O}(0.19), ν_{C5-O}(0.13), ν_{C-O}, ν_{C-C}(0.24)
1104	1106	1102	1102	ν_{C3-O}(0.29), ν_{C1-O}(0.2), δ_{CO2H}(0.07), ν_{C-O},$_{C-C}$(0.3)
1114	1124	1116	1117	ν_{C2-O}(0.21), ν_{C5-C6}(0.11), δ_{C1O1H}(0.25)
1122	1140	1130	1131	ν_{C2-O2}(0.18), ν_{C1-O}(0.17), ν_{C4-O}(0.18), $\nu_{CC,CO}$(0.23)
1134	1156	1153	1143	δ_{CO6H}(0.2), δ_{CO3H}(0.12), ν_{C3-O}(0.13), ν_{C-O}(0.33)
1149	1163	1157	1173	δ_{COH}(0.59), ν_{C-O}(0.07)
	1190		1189	δ_{CO4H}(0.31), δ_{COH}(0.23), ν_{C-C}(0.16)
	1195		1195	δ_{CO2H}(0.41), δ_{COH}(0.12), $\nu_{CC,CO}$(0.16)
1203	1205	1206	1216	δ_{COH}(0.41), ν_{CO}(0.19), ν_{C-C}(0.18)
1222	1219	1226	1226	δ_{CO3H}(0.22), δ_{COH}(0.11), ν_{C-O}(0.12), ν_{C-C}(0.18)
	1223		1241	ν_{C5-O}(0.27), ν_{C1-O5}(0.12), δ_{COH}(0.12)
	1233	1257		δ_{CC4H}(0.3), δ_{CC5H}(0.08), $\delta_{OC6H,C6OH}$(0.1), ν_{C1-O5}(0.05)
		1267	1258	δ_{C3OH}(0.15), δ_{C2OH}(0.1), $\delta_{C4OH,CC4H}$(0.11), $\nu_{C1-O}5$(0.05)
1273	1281	1283	1280	δ_{CC2H}(0.24), tw_{C6H2}(0.20)
1282	1294		1291	tw_{C6H2}(0.32), δ_{CCH}(0.19)
1296	1320	1312	1319	δ_{C3H}(0.5), δ_{C5H}(0.12), δ_{OCH}(0.15)
1331	1335		1333	wag_{C6H2}(0.43), ν_{C6-O}, ν_{C1-O5}(0.14)
1339	1350	1360	1345	δ_{CCH}(0.46), ν_{C1-O}(0.15)
1371	1393	1380	1380	$\delta_{CCH,OCH}$(0.51)
1378	1414	1385	1412	$\delta_{C3H,C4H}$(0.38), ν_{C-C}(0.12)
1406	1430	1412	1419	δ_{C1H}(0.49)
	1438		1428	sci_{C6H2}(0.65)
1428	1439		1438	$\delta_{CCH,COC}$(0.44), ν_{C-C}(0.12)
1443	1446	1451	1441	δ_{C5H}(0.21), sci_{C6H2}(0.27)
1459	1463		1488	$\delta_{CCH,COH}$(0.41), ν_{C-C}(0.12)
	2872	2878	2874	νs_{C6H2}
2877	2900		2901	νa_{C6H2}
	2918	2913	2918	ν_{C5-H}(0.57)
	2923	2935	2923	ν_{C2-H}(0.58)
	2932		2933	ν_{C4-H}, ν_{C2-H}
	2943		2942	ν_{C3-H}(0.50), ν_{C4-H}(0.35)
	2956	2950	2960	ν_{C1-H}(1.0)
	3397	3339	3398	ν_{O3-H}(0.72)
3791	3401	3381	3401	ν_{O6-H}(0.89)
	3405		3404	ν_{O2-H}(0.76)
	3407		3410	ν_{O4-H}(0.66)
3818	3409	3416	3414	ν_{O1-H}(0.76)
rms(cm^{-1})	17.8		19	

[a] The experimental frequencies are given for α-glucose; rms are given for wavenumbers < 1500 cm^{-1}.

et al.[18] The geometrical parameters and force constants have been derived from these studies. All parameters related to these different chemical groups have been included in a particular parameter file.

V. Conclusion

The SPASIBA force field has been parametrized for a large variety of chemical groups. The present work was devoted to the inclusion of these specific parameters into the CHARMM program. It has been shown that the refinement of the force field parameters using the spectroscopic data leads to a better prediction of various physical properties leading particularly to confidence when used in molecular dynamics simulations of molecules with biological interest including various chemical groups such as peptido-glycans or phospholipids.

Acknowledgment. P. Lagant, D. Nolde, and G. Vergoten are grateful to NATO for the support through the Collaboratory Linkage Grant NATO LST/CLG 978878.

References and Notes

(1) Derreumaux, P.; Vergoten, G. *J. Chem. Phys.* **1995**, *102* (21), 8586.
(2) Vergoten, G.; Mazur, I.; Lagant, P.; Michalski, J. C.; Zanetta, J. P. *Biochimie* **2003**, *85*, 65.
(3) Weiner, S. J.; Kollman, P. A.; Nguyen, D. A.; Case, D. T *J. Comput. Chem*. **1986**, *7*, 230.
(4) MacKerell, A. D., Jr.; Bashford, D.; Bellott, R. L.; Dunbrack, R. L., Jr.; Evanseck, J. D.; Field, M. J.; Fischer, S.; Gao, J.; Guo, H.; Ha, S.; Joseph-McCarthy, D.; Kuchnir, L.; Kuczera, K.; Lau, F. T. K.; Mattos, C.; Michnick, S.; Ngo, T.; Nguyen, D. T.; Prodhom, B.; Reiher, W. E., III; Roux, B.; Schlenkrich, M.; Smith, J. C.; Stote, R.; Straub, J.; Watanabe, M.; Wiorkiewicz-Kuczera, J.; Yin, D.; Karplus, M. *J. Phys. Chem. B.* **1998**, *102*, 3586.
(5) Shimanouchi, T.; Koyama, Y.; Itoh, K *Prog. Polym. Sci. Jpn*. **1974**, *7*, 273.
(6) Derreumaux, P.; Dauchez, M.; Vergoten, G. *J. Mol. Struct*. **1993**, *295*, 203.
(7) Derreumaux, P.; Vergoten, G. *J. Mol. Struct.* **1993**, *295*, 223.
(8) Derreumaux, P.; Vergoten, G. *J. Mol. Struct.* **1993**, *295*, 233.
(9) Tristram, F.; Durier, V.; Vergoten, G. *J. Mol. Struct*. **1996**, *377*, 47.
(10) Chhiba, M.; Tristram, F.; Vergoten, G. *J. Mol. Struct*. **1997**, *405*, 113.
(11) Chhiba, M.; Vergoten, G. *J. Mol. Struct*. **1994**, *326*, 35.
(12) Tristram, F.; Durier, V.; Vergoten, G. *J. Mol. Struct.* **1996**, *378*, 249.
(13) Dauchez, M.; Derreumaux, P.; Vergoten, G. *J. Comput. Chem.* **1992**, *14*, 263.
(14) Chhiba, M.; Derreumaux, P.; Vergoten, G. *J. Mol. Struct*. **1994**, *317*, 171.
(15) Chhiba, M.; Vergoten, G. *J. Mol. Struct.* **1996**, *384*, 55.
(16) Ledauphin, V.; Vergoten, G. *Biopolymers* **2000**, *57*, 373.
(17) Zanoun, A.; Durier, V.; Belaidi, A.; Vergoten, G. *J. Mol. Struct.* **1999**, *476*, 261.
(18) Durier, V.; Zanoun, A.; Belaidi, A.; Vergoten, G. *J. Mol. Struct.* **1999**, *476*, 271.
(19) Kitano, M.; Fukuyama, T.; Kuchitsu, K. *Bull. Chem. Soc. Jpn*. **1973**, *46*, 384.
(20) Katz, J. L.; Post, B. *Acta Crystallogr*. **1960**, *13*, 264.
(21) Hamzaoui, F.; Baert, F. *Acta Crystallogr*. **1994**, *C50*, 757.
(22) Guo, H.; Karplus, M. *J. Phys. Chem.* **1994**, *98*, 7104.
(23) Cornell, W. D.; Cieplak, P.;Bayly, C. I.; Gould, I. R.; Merz, K. M., Jr.; Ferguson, D. M.; Spellmeyer, D. C.; Fox, T.; Cadwell, J. W.; Kollman, P. A. *J. Am. Chem. Soc*. **1995**, *117*, 5179.
(24) Ataka, S.; Takeuchi, M.; Tasumi, H. *J. Mol. Struct*. **1984**, *113*, 147.
(25) Madison, V.; Kopple, K. D. *J. Am. Chem. Soc.* **1980**, *102*, 4855.
(26) Tobias, D. J.; Brooks, C. L., III. *J. Phys. Chem*. **1992**, *96*, 3864.
(27) Schachtschneider, J. H.; Snyder, R. G. *Spectrochim. Acta* **1963**, *19*, 117.
(28) Oyagami, K.; Kutchitsu, K *Bull. Chem. Soc. Jpn.* **1978**, *51*, 2237.
(29) Hayashi, M.; Adachi, M. *J. Mol. Struct.* **1982**, *78*, 53.
(30) Perchard, J. P.; *Spectrochim. Acta, Part A.* **1970**, 707.
(31) Smith, D.; Devlin, J. P.; Scott, D. W. *J. Mol. Spectrosc.* **1968**, *25*, 174.
(32) Bloom, C. E.; Gunthard, H. H. *Chem. Phys. Lett.* **1981**, *84*, 267.
(33) Barnes, 1.J.; Howells, J. D. R. *J. Chem. Soc., Faraday Trans 2* **1973**, *69*, 532.
(34) Lide, D. R.; Mann, D. E. *J. Phys. Chem.* **1957**, *27*, 868.
(35) Kimura, M.; Kubo, K. *J. Chem. Phys*. **1959**, *30*, 151.
(36) Lees, R. M.; Baker, J. G. *J. Chem. Phys.* **1968**, *48*, 5209.
(37) Serralach, A.; Meyer, R.; Gunthard. H. H. *J. Mol. Spectrosc*. **1974**, *52*, 94.
(38) Schaefer, L. *J. Mol. Struct.: THEOCHEM* **1982**, *86*, 349.
(39) Durier, V.; Lagant, P.; Kirillova, S.; Vergoten, G. To be submitted for publication.
(40) Kitamura, S.; Minami, T.; Nakamura, Y.; Isuda, H.; Kobayashi, H.; Mimura, M.; Urakawa; Kajiwara, K.; Ohno, S. *J. Mol. Struct.*: THEOCHEM **1997**, *395*−*396*, 425.
(41) French, A. D.; Kelterer, A. M.; Johnson, G. P.; Dowd, M. K.; Cramer, C. J. *J. Mol. Graphics Modell.* **2000**, *18*, 95.